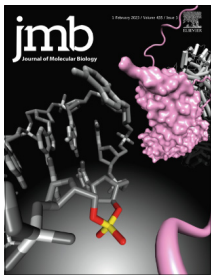

Drosophila Me31B is a Dual eIF4E-Interacting Protein

Carla Layana [1*], Emiliano Salvador Vilardo [1†], Gonzalo Corujo [1‡], Greco Hernández [2] and Rolando Rivera-Pomar [1,3,4]

***1* - Centro Regional de Estudios Genómicos,** *Facultad de Ciencias Exactas, Universidad Nacional de La Plata, Boulevard 120 Nº 1459, 1900 La Plata, Argentina*

***2* - Translation and Cancer Laboratory,** *Unit of Biomedical Research on Cancer, National Institute of Cancer (Instituto Nacional de Cancerología, INCan), 22 San Fernando Ave., Tlalpan, 14080 Mexico City, Mexico*

***3* - Centro de Investigación y Transferencia del Noroeste de Buenos Aires (CITNOBA) – Centro de Bioinvestigaciones,** *Universidad Nacional del Noroeste de Buenos Aires, Av. Presidente Frondizi Km 4, 2700 Pergamino, Argentina*

***4* - Molecular Developmental Biology Emeritus Group,** *Max Planck Institute for Multidisciplinary Sciences, Am Fassberg 11, 37077 Göttingen, Germany*

Correspondence to Carla Layana: *clayana@conicet.gov.ar (C. Layana)*
https://doi.org/10.1016/j.jmb.2023.167949
Edited by Ruben L. Gonzalez

Abstract

Eukaryotic translation initiation factor 4E (eIF4E) is a key factor involved in different aspects of mRNA metabolism. *Drosophila melanogaster* genome encodes eight eIF4E isoforms, and the canonical isoform eIF4E-1 is a ubiquitous protein that plays a key role in mRNA translation. eIF4E-3 is specifically expressed in testis and controls translation during spermatogenesis. In eukaryotic cells, translational control and mRNA decay is highly regulated in different cytoplasmic ribonucleoprotein foci, which include the processing bodies (PBs). In this study, we show that *Drosophila* eIF4E-1 and eIF4E-3 occur in PBs along the DEAD-box RNA helicase Me31B. We show that Me31B interacts with eIF4E-1 and eIF4E-3 by means of yeast two-hybrid system, FRET in *D. melanogaster* S2 cells and coimmunoprecipitation in testis. Truncation and point mutations of Me31B proteins show two eIF4E-binding sites located in different protein domains. Residues Y401-L407 (at the carboxy-terminus) are essential for interaction with eIF4E-1, whereas residues F63-L70 (at the amino-terminus) are critical for interaction with eIF4E-3. The residue W117 in eIF4E-1 and the homolog position F103 in eIF4E-3 are necessary for Me31B-eIF4E interaction suggesting that the change of tryptophan to phenylalanine provides specificity. Me31B represents a novel type of eIF4E-interacting protein with dual and specific interaction domains that might be recognized by different eIF4E isoforms in different tissues, adding complexity to the control of gene expression in eukaryotes.

Introduction

Translation is the most dynamic process to regulate the composition and quantity of the cell proteome. Translational control enables rapid changes in the translatability of mRNAs in response to environmental, physiological, and developmental clues.[1,2] Part of this regulation occurs in large, membrane-less aggregates of proteins and non-translating mRNAs termed mRNP

granules or cytoplasmic foci. RNP granules accumulate multivalent protein–protein, RNA–RNA, and protein–RNA with specific biochemical properties that define the nature of the granules.[3] The different cytoplasmic foci include processing-bodies (PBs), present in most eukaryotic cells, stress granules (SGs), which form upon stress stimuli, germ granules (GGs), and neuronal granules (NGs), among others.[4–6]

Messengers, when they are not translated, can be transiently stored or even degraded in some of these granules, including PBs. PBs occur in normal cells but can be further increased under a variety of stress conditions.[4–6] PBs contain the mRNA decay machinery and, accordingly, contain enzymes involved in RNA degradation, do not present exosome components nor ribosomal proteins or translation factors.[4–6] Indeed, a mutually excluding functional relationship between PBs and translation regulation has been demonstrated, as drugs that block polysomes dynamic (e.g., puromycin) promote the assembly of PBs.[7–9] Intriguingly, and despite PBs contain translationally repressed mRNAs, the only translation initiation factor present in these granules is the eukaryotic translation initiation factor 4E (eIF4E). In mammals,[10–13] *Xenopus*,[14] the protozoan *Trypanosoma brucei*,[15] the planaria *Dugesia japonica*,[16] *Saccharomyces cerevisiae*,[17–18] *Drosophila melanogaster*,[8,19] and *Caenorhabditis elegans*,[20] eIF4E occurs in PBs.

eIF4E recognizes the cap structure at the 5′ end of the mRNAs. Along with the scaffold protein eIF4G and the DEAD-box ATP-dependent RNA helicase eIF4A, eIF4E forms the eIF4F complex. eIF4F promotes cap-dependent translation initiation mediating the interaction between the mRNA and the ribosomes to form the 43S ribosomal preinitiation complex.[21,22] Evidence is mounting that eIF4E also plays critical roles in mRNA transport, storage, and translational repression in cytoplasmic foci.[23] In *Xenopus* and human cells, translation of mRNAs is repressed in PBs when eIF4E interacts with eIF4E-transporter (4E-T)[10,11] and with DEAD-box ATP-dependent RNA helicase rck/p54 (humans)[11] or its *Xenopus* ortholog Xp54,[14] another component of PBs. In addition, other low-abundance eIF4E isoforms, such as 4EHP, may play different translation-regulating roles in different tissue or cellular contexts.[24]

A key role in translational repression also has been established for the *D. melanogaster* ortholog of rck/p54 and Xp54, namely Maternal expression at 31B (Me31B). Me31B is a member of a highly conserved superfamily 2/DDX6 of DEAD-box RNA helicases with roles in translational repression from trypanosomes to humans.[25,26] Along with the RNA-binding protein Tral, the mRNA 3´-UTR-binding protein Orb, the eIF4E-binding protein Cup, and the RNA localization factor Exuperantia (Exu), Me31B assembles with mRNAs to form translationally repressed mRNPs in germ granules and PBs.[19,27–29] During oogenesis, Me31B down-regulation results in premature translation of *oskar* and *bicoid* mRNAs in nurse cells.[30] Moreover, Wang et al.[31] showed that Me31B is a general regulatory factor that binds to and represses the expression of thousands of maternal mRNAs during the maternal-to-zygotic transition.[31] Because Me31B is expressed in different tissues throughout *D. melanogaster* development, i.e., nurse cells, oocytes, and early embryos, and accumulates in diverse RNP granules, such as PBs, germ plasm granules, nuage granules, and sponge bodies,[19,32,27–30] Wang et al. suggested that the repressive capabilities of Me31B depend on the different biological context in which it occurs.[31] PBs formation and function require protein–protein interactions and inactive mRNAs. However, an unresolved issue is how PBs can store specific mRNAs. It might involve multiple signals and proteins, some common for the whole transcriptome and some specific to a particular mRNA.[33] Thus, to better understand the role of Me31B in different cell processes, it is crucial to determine their interaction partners.

In this study, we analyzed the interaction of Me31B with the isoforms eIF4E-1 and eIF4E-3 in *D. melanogaster* in PBs. We show that residues at the carboxy-terminal of Me31B (Y401-L407) are essential for interaction with eIF4E-1, while residues near the amino terminus (F63-L70) are required for the interaction with eIF4E-3, representing a novel structure of an eIF4E-interacting protein. Our results provide further evidence to the hypothesis that alternative paralogs of eIF4E and their interactions add complexity to the control of gene expression in eukaryotic cells.

Results

Different eIF4E isoforms and Me31B are present in PBs in D. melanogaster

We investigated Me31B by transfection of S2 cells with the fusion proteins YFP-Me31B or CFP-Me31B and by immunofluorescence. We detected Me31B in cytoplasmic foci that we attributed as PBs as Me31B colocalizes with GW182, a marker of PBs (Figure 1(A)). In contrast, in cells stressed with sodium arsenite, we could not detect the colocalization of Me31B with Rox8 (TIA-1), a stress granule marker (Figure 1(B)). The results of the colocalization analysis are summarized in Figure S1 and Table S1. Me31B fluorescent proteins are detected in discrete PBs, although a fraction remains dispersed in the cytoplasm (Figure 1(C)). It is important to note that only some cells show endogenous Me31B granules, while other ones do not express the protein or express it at low level. This is likely due to the heterogeneous nature of S2 cell line, which

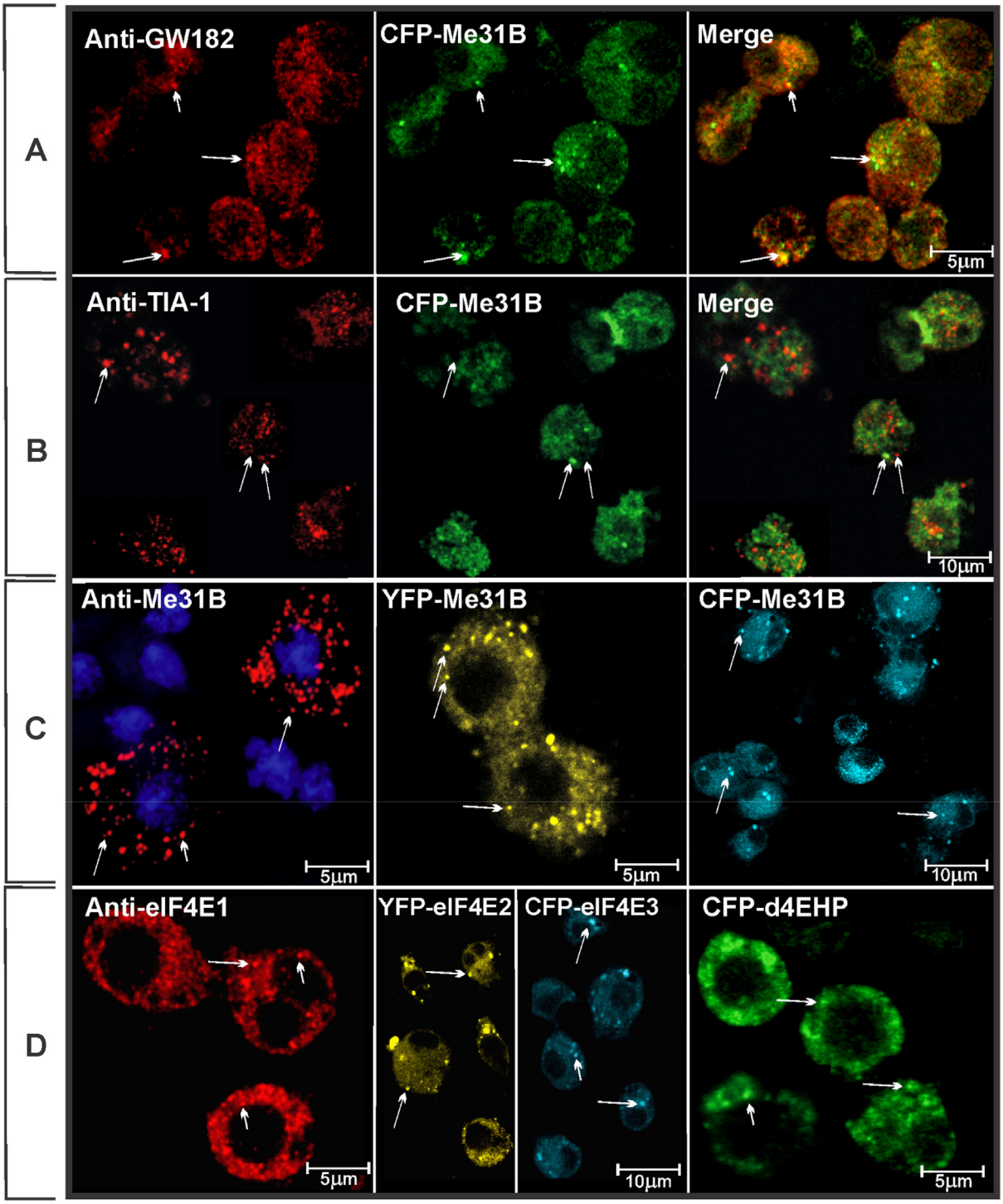

Figure 1. Localization of Me31B and eIF4Es in PBs. (A, B) Me31B localizes in PBs but not stress granules. S2 cells were transfected with fluorescent protein constructs (CFP-Me31B) and immunostained with the indicated antibodies. Anti-GW182 antibody was used as PBs marker (A) and anti-TIA-1 antibody as a marker of stress granules (B). In (B) cells were incubated for 30 min with 1 mM sodium arsenite before fixation. Merge images show Me31B accumulation in PBs (*white arrows*). In contrast, stress granules that contain TIA-1 did not merge with CFP-Me31B (*white arrows*). (C, D) S2 cells were either immunostained with the indicated antibodies or transfected with fluorescent protein constructs (YFP- or CFP-), as indicated. (C) Me31B. In all cases, the indicated proteins accumulated in PBs. (D) From left to right: eIF4E-1, eIF4E-2, eIF4E-3 and d4E-HP. Examples of PBs contain the proteins are marked with arrows.

derives from *D. melanogaster* late embryos,[34] that are composed of different cellular lineages.

We observed that Me31B also aggregates in cytoplasmic granules that lack GW182 and, similarly, we found granules with GW182 lacking Me31B. This suggests that cytoplasmic granules are a polymorphic family in which different functions and/or maturation stages might be simultaneously represented in the cells, as it has been proposed before.[35] Additional evidence suggests that these dynamic structures could mature in SG, the formation of PB could precede the formation of SG.[35,36]

In *Drosophila* seven *eIF4E* paralog genes encode eight protein isoforms, namely eIF4E-1, eIF4E-2, eIF4E-3, eIF4E-4, eIF4E-5, eIF4E-6, eIF4E-7 and d4EHP/eIF4E-8.[37] We studied four eIF4E isoforms in *Drosophila* S2 cells, either with a specific antibody against the isoform eIF4E-1 or as fusion proteins in the case of YFP-eIF4E-2, YFP-eIF4E-3 and CFP-d4EHP (Figure 1(D)). In all cases we detected the occurrence of eIF4E in cytoplasmic foci.

It has been shown that eIF4E and rck/p54 colocalize in vertebrate cells.[11] Therefore, we studied whether the *Drosophila* orthologous proteins, eIF4E and ME31B colocalize in S2 cells. We co-transfected the cells with plasmids encoding the fluorescent fusion proteins YFP-Me31B and CFP-eIF4E-3. The intensity profile across one PBs showed that colocalization is specific in cytoplasmic granules (Figure 2). The same analysis was performed with the pair CFP-Me31B and YFP-eIF4E-1, and it was also found that both colocalize in PBs. Both YFP-eIF4E-2 and YFP-d4EHP fusion proteins are colocalized with CFP-Me31B as well (Figure S2 and Table S1). These results suggested that Me31B colocalizes with different isoforms of eIF4E in cytoplasmic foci, which led us to consider they play a role in PBs formation. Me31B function in germ line development,[38,39] therefore we further studied the interaction with the eIF4E isoforms that simultaneously occur in the male germ line, namely eIF4E-1[40] and eIF4E-3.[41]

Me31B interacts with eIF4E-1 and eIF4E-3

We first performed two-hybrid assays in yeast using Me31B as "prey" and eIF4E-1 and eIF4E-3 as "baits" (Figure 3(A)). As positive control we used *D. melanogaster* eIF4E-BP and PABP as negative control.[37] Diploid cells derived from mating cells containing either bait and prey plasmids were grown in selective media (–Trp, –Leu) as control. Protein-protein interactions were detected by replica-plating diploid cells onto selective media (-Trp, -Leu, -His) containing 12 mM 3-amino-1,2,4-triazole (3AT). We observed that Me31B interacts with both eIF4E-1 and eIF4E-3 in the selective medium.

We further evaluated if the protein–protein interaction occurs in the S2 cells cytoplasmic granules using fluorescence resonance energy transfer (FRET). We tagged Me31B, eIF4E-1, and eIF4E-3 with CFP as acceptor and YFP as donor.[42] FRET efficiency was measured by acceptor photobleaching, which implies that the acceptor quenches the donor fluorescence as the excitation energy is transferred to the acceptor, but after photobleaching of the acceptor, the quenching is blocked, and the donor fluorescence increases. Quantification of the increase is a reliable and

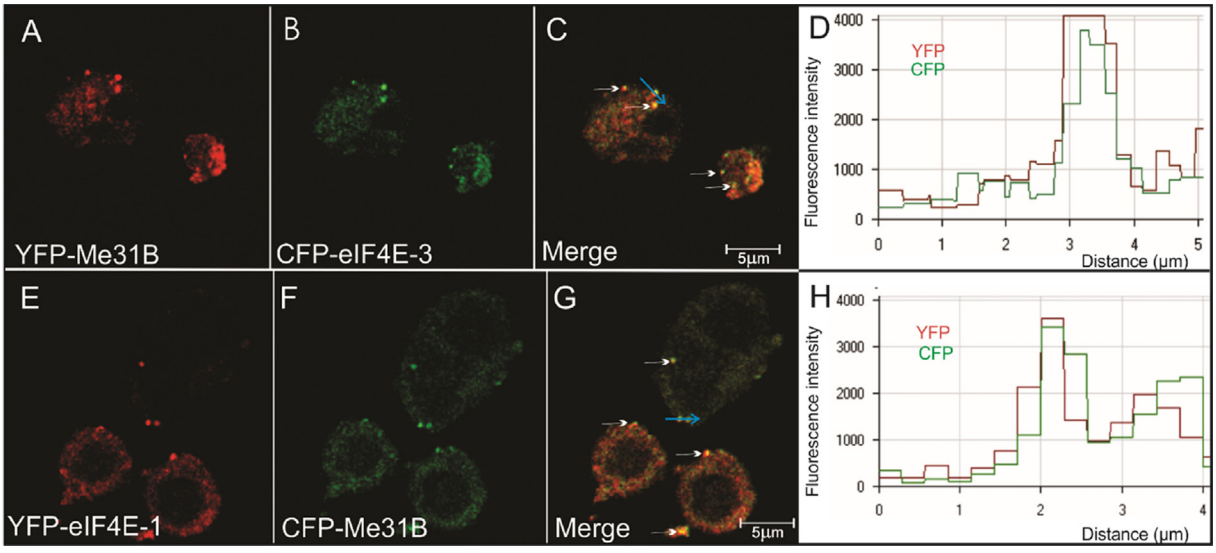

Figure 2. Me31B colocalize with eIF4E-1 and eIF4E-3 in PBs. Processing bodies of S2 cells transfected with fluorescent fusion proteins contain Me31B (A), eIF4E-3 (B) and eIF4E-1 (E). In merge image (C, G) we can see both proteins are located in the same granules. (D, H) Intensity profile of CFP and YFP fluorescence as a function of the distance that a PB crosses (blue arrow in C and G). Examples of colocalization are marked with white arrows.

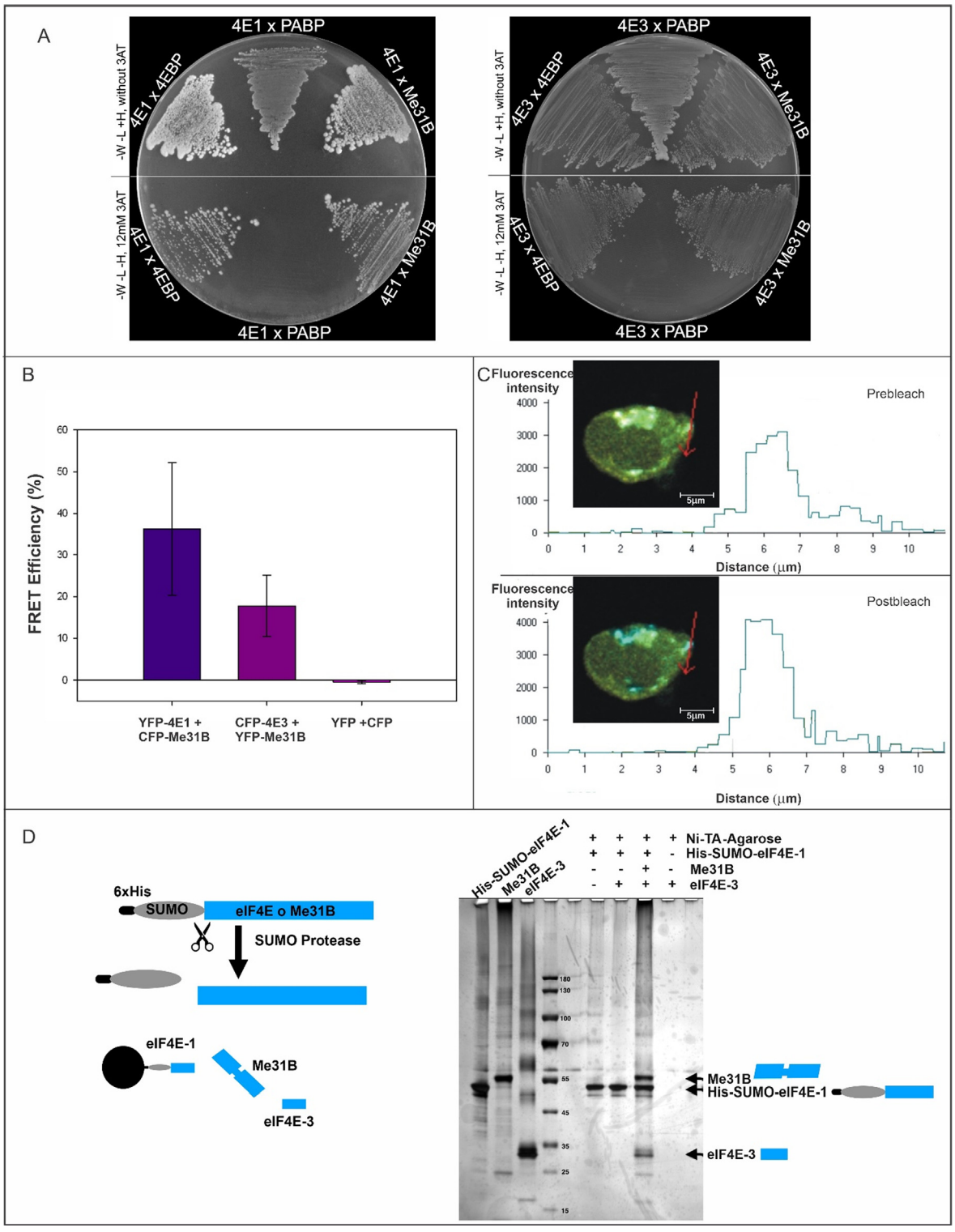

Figure 3. Me31B interacts with eIF4E-1 and eIF4E-3. (A) Yeast two-hybrid system. 4E-BP was used as a positive control and PABP as a negative control. *L*, leucine; *W*, tryptophan; *H*, histidine; *3AT*, 3-amino-1,2,4-triazole. (B) FRET in S2 cells. Bar charts represent the mean values of the apparent FRET efficiencies of protein pairs from several PBs in different cells. Error bars indicate the standard deviation from the mean values. Confocal images of both CFP and YFP channels were taken before and after photobleaching (C). Intensity profile of the CFP fluorescence before and after photobleaching as a function of the distance (*red arrow*) crossing a PB. CFP fluorescence increased after bleaching because the acceptor is absent. (D) Copurification assay with recombinant proteins. The arrows indicate each component (His-tagged eIF4E-1, Me31B and eIF4E-3).

robust measure of FRET.[43,44] Cells expressing CFP/YFP pairs of tagged eIF4E-1 and Me31B showed an average FRET efficiency of 36%, and cells expressing fluorescent tagged eIF4E-3 and Me31B showed an average FRET efficiency of 25%. In contrast, cells expressing only CFP and YFP (negative control) did not show significant FRET level (Figure 3(B)). Figure 3(C) shows a color image of a cell co-expressing YFP-eIF4E-1 and CFP-Me31B pre and post bleached PB. In post-bleached images, we observed a diminution of the intensity of donor molecules (YFP, yellow). We show the intensity profile of CFP fluorescence before and after photobleaching, depending on the distance through the red arrow, which crosses one bleached PB. After photobleaching, CFP-fluorescence was incremented because the acceptor was absent, and the energy transfer to acceptor did not happen. The non-bleached PBs did not exhibit FRET.

Our data support the notion that Me31B is an eIF4E-interacting protein that targets eIF4E-1 and eIF4E-3 *in vivo* and that the interaction is binary and direct. We then investigated if the interaction of Me31B with eIF4E-1 and eIF4E-3 can be simultaneous. Co-immunoprecipitation of endogenous proteins using anti-eIF4E-1 antibody in S2 cells showed the presence of eIF4E-3 and Me31B wich indicates the interaction with eIF4E3 and Me31B (Figure S3). To further confirm the results, we expressed and purified the three proteins in bacteria (see methods for details) and performed a copurification assay using NiTA-agarose, His-tagged eIF4E-1 and untagged Me31B and eIF4E-3 (Figure 3(D)). We incubated the components and separated the ones bound to the solid support by SDS-PAGE. eIF4E-3 is retained to the immobilized eIF4E-1 only in the presence of Me31B, indicating that at least a fraction of Me31B can simultaneously interact with both eIF4E-1 and eIF4E-3.

Different domains of Me31B interact with eIF4E-1 and eIF4E-3

In *D. melanogaster* eIF4E-1, the residues W100 and W146 are required for cap recognition and are involved in translation initiation, while W117 (W73 in human eIF4E) is required for protein–protein interactions and participates in translation repression and PBs assembly.[8] F103 in eIF4E-3 is equivalent to W117 in eIF4E-1. We had previously demonstrated that the mutants eIF4E-3^{F103A} and eIF4E-1^{W117A}, do not localize in PBs.[9] We performed yeast two-hybrid assay and observed that W117 in eIF4E-1 and F103 in eIF4E-3 are required to interact with Me31B (Figure 4). These results suggest that the interaction between Me31B and eIF4E-1 and eIF4E-3 might be required to recruit them to PBs, most likely to silence mRNAs. Me31B is composed of two linked RecA-like domains, domains 1 (D1) and 2 (D2).[14] D1 contains the Q motif followed by motifs I–III, and D2 contains motifs IV–VI participate in ATP binding and RNA binding (Figure 5(D)). As we have shown that the interaction can be simultaneous, we investigated whether eIF4E-interactions are mediated by different domains of Me31B.

We used the yeast two-hybrid system assays to analyze the interaction of truncated Me31B with

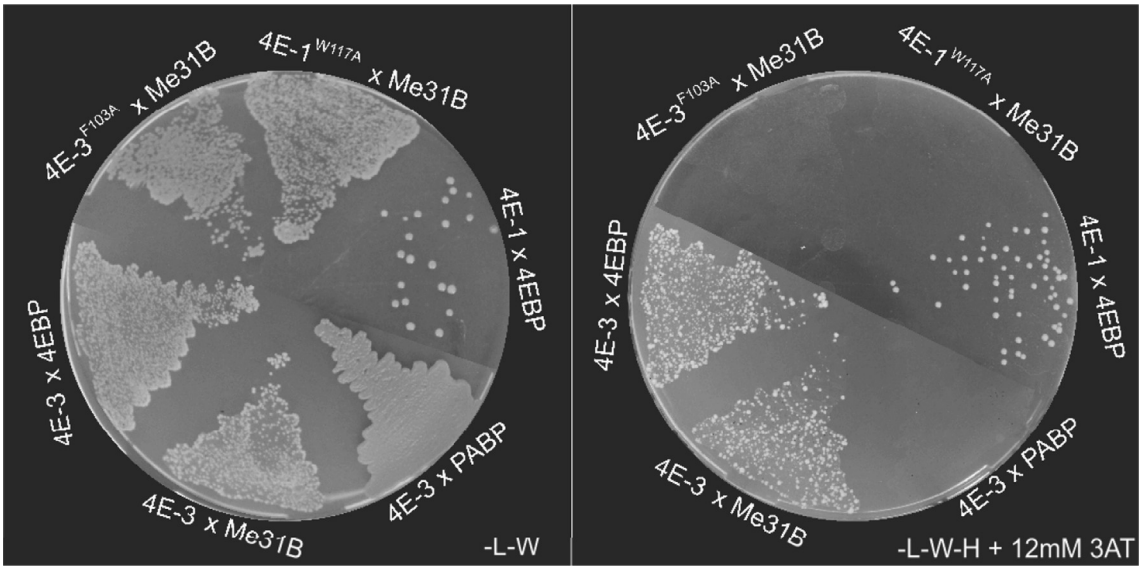

Figure 4. Mutants of eIF4E at essential sites for accumulation in PBs do not interact with Me31B. eIF4E-1^{W117A} and eIF4E-3^{F103A} do not interact with Me31B in the yeast two-hybrid system. *Left:* mating control plate. 4E-BP was used as a positive control and PABP as a negative control. *L*, leucine; *W*, tryptophan; *H*, histidine; *3AT*, 3-amino-1,2,4-triazole.

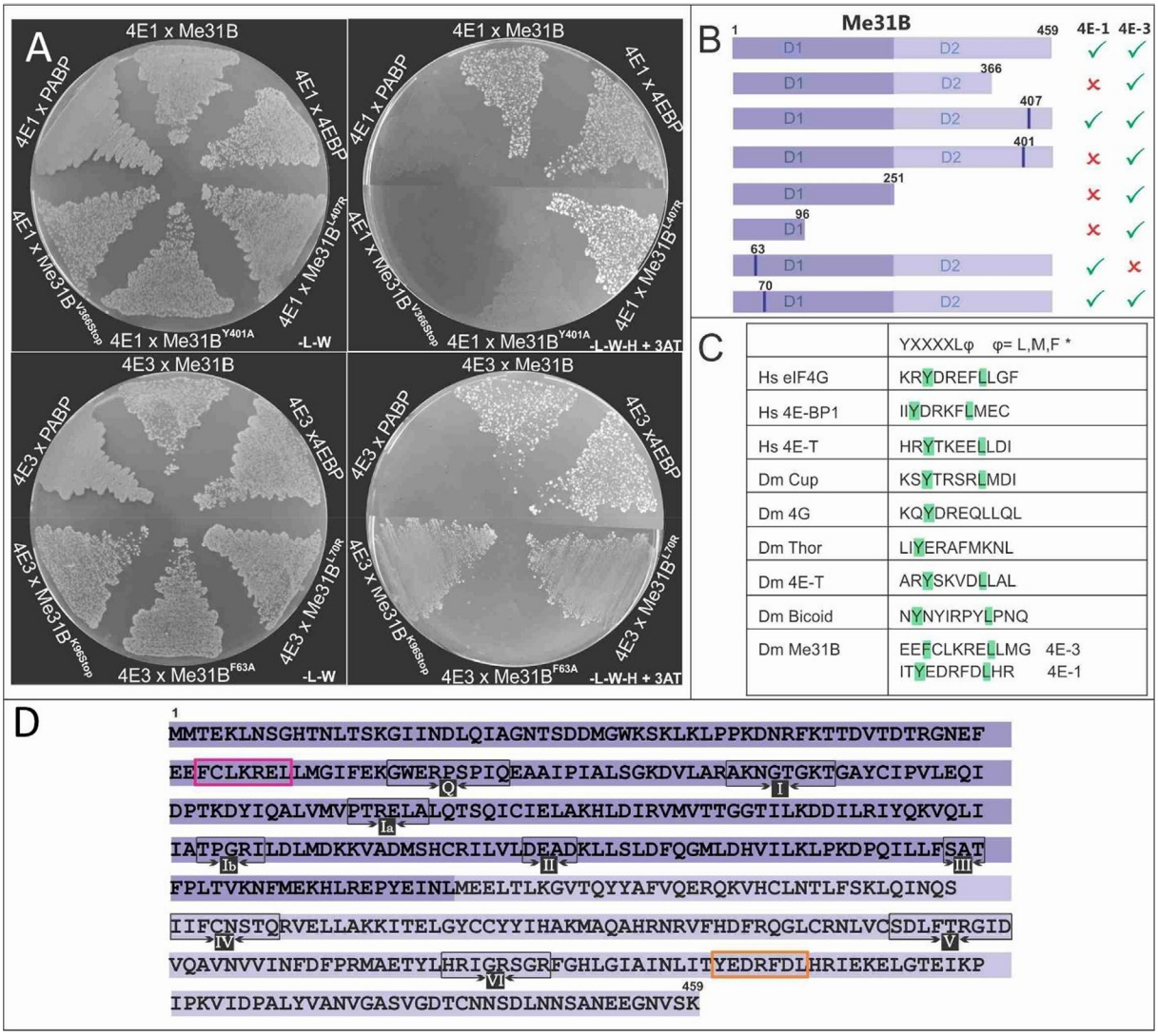

Figure 5. Two independent domains of Me31B interact with eIF4E-1 and eIF4E-3. (A) Yeast two-hybrid assays with Me31B mutants. *Left*, mating control plate. 4E-BP was used as a positive control and PABP as a negative control. *L*, leucine; *W*, tryptophan; *H*, histidine; *3AT*, 3-amino-1,2,4-triazole. (B) Me31B protein fragments are represented as *bars*. D1 and D2 domains are highlighted in *dark purple* and light purple, respectively. Different mutants were evaluated for interaction. *Crosses* indicate no interaction, and *ticks* indicate positive interactions. (C) Consensus sequences of the eIF4E-binding motif (4E-BM) from the indicated eIF4E-interaction proteins. Me31B 4E-BMs found in this study are also shown. (D) Me31B sequence. Interaction sites with eIF4E-1 and eIF4E-3 are marked in *orange* and *pink*, respectively.

both eIF4E-1 and eIF4E-3 isoforms. We mutated the codons V366, C285, K251, K194, K124, and K96 to a stop codon to generate truncated versions of Me31B (Figure 5(B) and Figure S4). Our results show that the binding sites of Me31B for eIF4E-3 and eIF4E-1 are located in different domains of Me31B. eIF4E-3 binds to D1 domain ($Me31B^{1\text{-}96}$) whereas eIF4E-1 with D2 domain ($Me31B^{366\text{-}459}$) (Figure 5(A, B)). We next searched for the eIF4E-binding sites (4E-BSs) present in Me31B. Most eIF4E-interacting proteins display the canonical interaction domain of eIF4G (YxxxxLφ),[45] however, there are exceptions, some use a different but similar domain such as Bicoid[46] and others do not use the consensus domain such as Importin 8.[47] Two canonical motifs (YxxxxLφ) were found within the domains D1 and D2 of Me31B (Figure 5(C)). To test the functionality of these sites, we performed site-directed mutagenesis to replace residues F63 to alanine and L70 to arginine in the eIF4E-3 putative interacting region and Y401 to alanine and L407 to arginine in the eIF4E-1 putative interacting site. The substitution of both aromatic residues Y401 and F63 to non-aromatic ones abolished the interaction of Me31B with eIF4E-1 and eIF4E-3, respectively (Figure 5

(A, B)). It is noteworthy that the Me31B mutants for one interaction site are still functional to interact through the non-mutated site with the corresponding eIF4E isoform. Therefore, we conclude that Me31B interacts with eIF4E-1 and eIF4E-3 through two independent binding sites specific for each isoform.

To determine if the interaction sites are also required for localization of Me31B we next studied the cellular distribution of Me31B mutants. S2 cells were transfected with a plasmid expressing CFP-Me31B^{F63A}, CFP-Me31B^{Y401A} and CFP-Me31B as a control. The mutants that lack the amino acid essential for the interaction with eIF4E-1 and eIF4E-3 are homogeneously distributed in the cytoplasm and do not accumulate in foci, compared to wild type Me31B (Figure S5). This result supports our idea that the interaction between Me31B and eIF4E-1 and/or eIF4E-3 might be required to recruit the protein to PBs.

Expression of Me31B and eIF4E-3 in the male germ line

The function of Me31B has been well studied in the female germ line, but our knowledge in the male germ line is scarce. Me31B is expressed in the male germ line of *D. melanogaster* (Figure S6) as indicated by expression data (https://flybase.org/reports/FBgn0004419) and recent publications.[38,39] We studied the localization of Me31B in vivo using a transgenic line expressing a GFP-Me31B fusion that replaces the endogenous gene and fully rescues the phenotype. GFP-Me31B is detected at the tip of the testis in the stem cell niche and in the spermatogonia, where the initial mitotic divisions take place (Figure 6(A) and Figure S7). GFP-Me31B is coexpressed with the stem cell marker vasa in these cells (6B). In living cells, GFP-Me31B imaging shows cytoplasmic foci in stem cells (Figure 6(C)) and in primary spermatocytes (Figure 6(D)), cells that undergo transcription and regulated translation.[48]

Previous studies have shown that eIF4E-3 is expressed in *D. melanogaster* germline[41,49] and is essential for spermatogenesis. We observed that GFP-Me31B and eIF4E-3 are coexpressed in the male germline (Figure 7(B, C)). A quantitative analysis using the Manders coefficient supports the preferent colocalization in spermatocytes over stem cells (Table S1). Closer examination reveals that, as spermatogenesis proceeds, GFP-Me31B and eIF4E-3 are associated with meiotic figures (Fig-

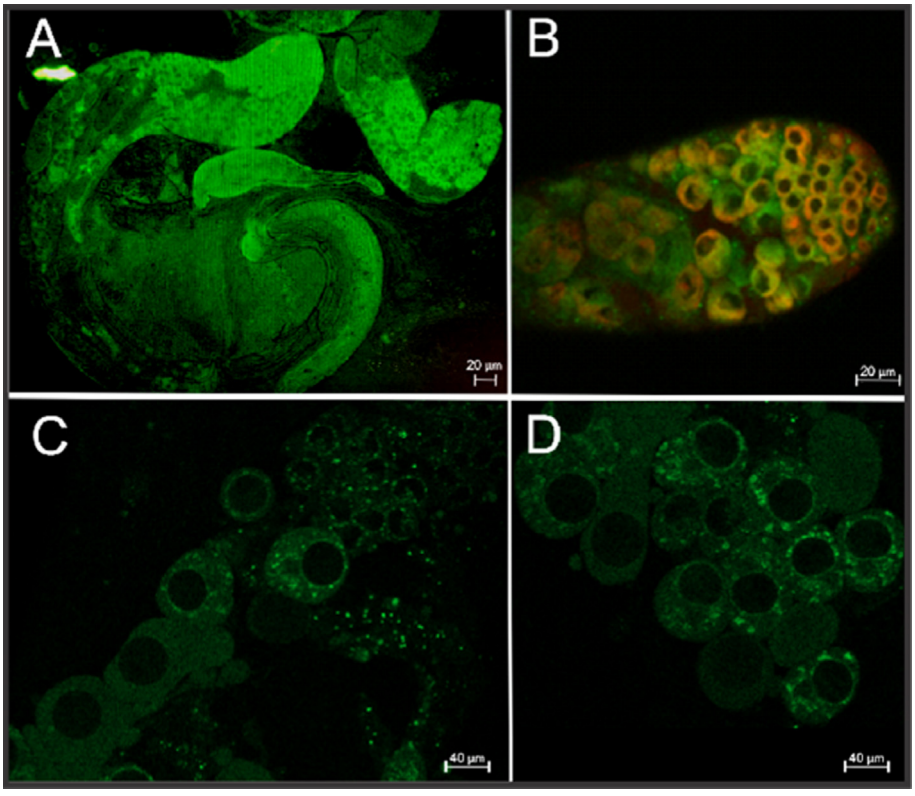

Figure 6. Me31B is found in male germ line. (A) Me31B is located in different cells type in testis of the trapline GFP-Me31B. (B) Immunofluorescence with anti-vasa (red) and anti-GFP antibodies (green). Both proteins are detecteded in the stem cells (Manders colocalization coefficient MA = 0.86 ± 0,02; MB = 0.74 ± 0,04). Me31B is observed in cytoplasmic granules in stem cells and spermatocytes (**C**, **D** respectively). The cells in **C** and **D** images were not fixed and they separated from the rest of the tissue by aspirating.

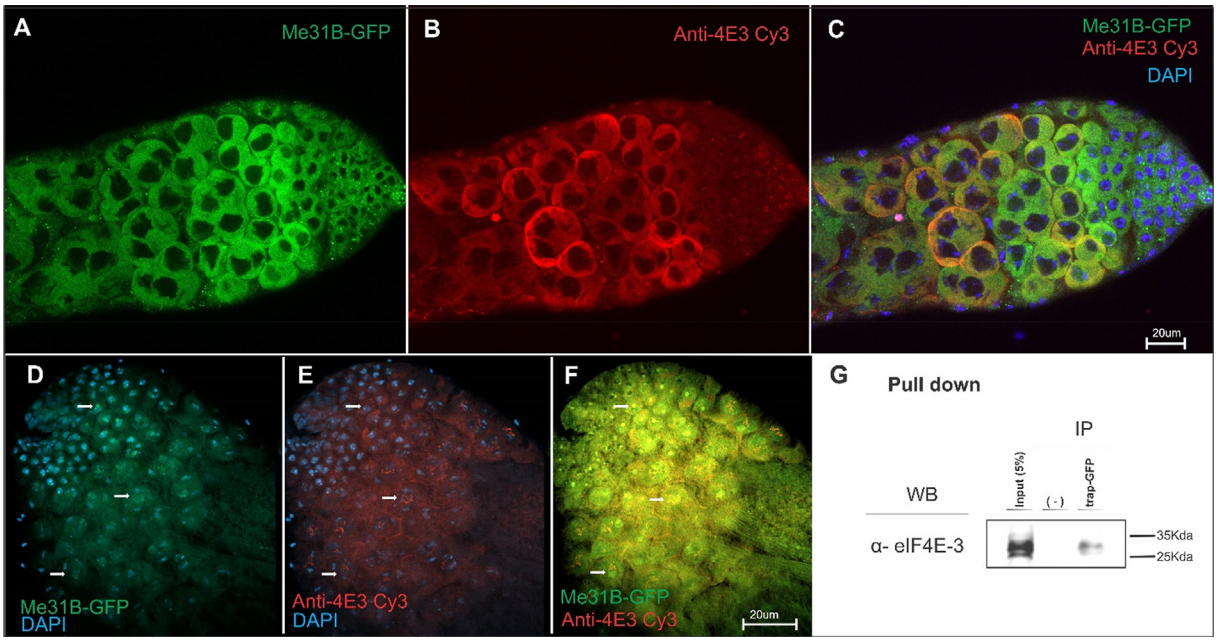

Figure 7. Me31B is detected in testis and colocalizes with eIF4E-3. (A) Me31B is observed located in stem cells and spermatocytes in testis of the trapline GFP-Me31B flies. (B) Testis immunofluorescence with anti-eIF4E-3 antibodies of GFP-Me31B flies. Both proteins are located in the same spermatocytes (C). The superposition of both fluorescence signals confirms colocalization (Manders coefficient MA = 0.85 ± 0.03; MB = 0.71 ± 0.02). (D, E) Me31B and eIF4E-3 are seen associated with meiotic chromosomes, DAPI staining is shown in blue. The co-location of both is shown in figure F. (G) Co-IP experiments showing that Me31B physically interacts with eIF4E-3 in testis. Total extracts of testes from GFP-Me31B flies were used to conduct immunoprecipitations using GFP-trap and interactions were detected by immunoblotting.

ure 7(F), white arrows). This agrees with the non-canonical function of eIF4E-3 in chromosome segregation[41] and opens a path for further studies for a non-canonical function of Me31B in the male germ line. Finally, to validate the interaction determined by FRET and yeast two hybrid assays in the male germ line, we performed a pull-down experiment with GFP-Me31B using anti-GFP nanobodies in isolated testis and showed the co-purification of eIF4E-3 (Figure 7(G)). Taken together, these results suggest that the function of Me31B in the male germline might require the interaction with eIF4E-3.

Discussion

Cytoplasmic mRNA granules can be found in a variety of configurations, depending on their protein composition. These structures play critical roles in post-transcriptional regulation of gene expression.[33,50] The interaction of *Drosophila* eIF4E-1 and eIF4E-3 with Me31B in PBs agrees with RNAi studies demonstrating that Me31B is necessary for PBs assembly.[51] Me31B also plays an essential role in translation regulation during oogenesis[30,52,53] and, as recently shown, in spermatogenesis.[39] Thus, Me31B along with other proteins, might be involved in mRNPs remodeling from active polysomes to repression by direct interaction with eIF4E. Translational control is a key issue in differentiation of male gametes, but our knowledge of the molecular mechanisms involved lag behind those in oogenesis.[54]

A model has been previously proposed by the removal of the translation machinery, mRNP reorganization, and PBs assembly.[33] eIF4E is the only translation factor present in active mRNAs and in the mRNP of PBs.[55] A common set of eIF4 factors support the basal translation initiation, whereas, at least in *D. melanogaster*, different eIF4E isoforms might regulate the translation in a tissue- and or developmental-specific manner.[56] *D. melanogaster* eIF4E-1 seems to be the canonical isoform,[37] while eIF4E-8/d4E-HP is a repressor of *bicoid* mRNA during embryogenesis,[46] eIF4E-4 has been reported to function in the cardiac tissue,[57] and eIF4E-3 is a testis-specific modulator of male germline development.[41,49]

In this study, we showed that eIF4E directly interacts with the helicase Me31B. We propose that this interaction is mutually exclusive with other 4E-BP such as eIF4G based in the aminoacids required for the interaction and hypothesize that it has a functional role in post-transcriptional regulation. However, while eIF4E-BP binds eIF4E-1, it does not bind eIF4E-3, raising the critical question of what protein or proteins regulate eIF4E-3.[41,49] We support the idea

that Me31B could compete with eIF4G to displace it from the interaction with eIF4E, and therefore, prevent translation. We showed that the mutants eIF4E-1^{W117A} and eIF4E-3^{F103A} are not assembled into PBs[8] and do not interact with Me31B supporting the idea that displacement of eIF4G might lead to the repression of mRNA into PBs.

Both Me31B 4E-binding sites are non-canonical 4E-BP motifs and it is plausible to consider that they interact with different eIF4E domains, as it was shown for the d4E-HP/Bicoid interaction.[46] Molecular modeling of Me31B shows that the interaction motifs at the D1 and D2 domains are far apart to allow simultaneous binding of eIF4E-1 and eIF4E-3, as our experimental evidence also suggests (Figure 8(A)). The interaction is mediated at least by F103 in eIF4E-3 and its equivalent position W117 in eIF4E-1. W117 is conserved in all *D. melanogaster* eIF4E isoforms, but eIF4E-3 (Figure 8 (B)), suggesting that the phenylalanine is enough to provide binding specificity to the D1 interacting site. Recent studies showed that some eIF4E-interacting proteins need two domains to interact with the same eIF4E molecule, namely one canonical 4E-BS that interacts with the dorsal surface of eIF4E, and a non-canonical one that interacts with

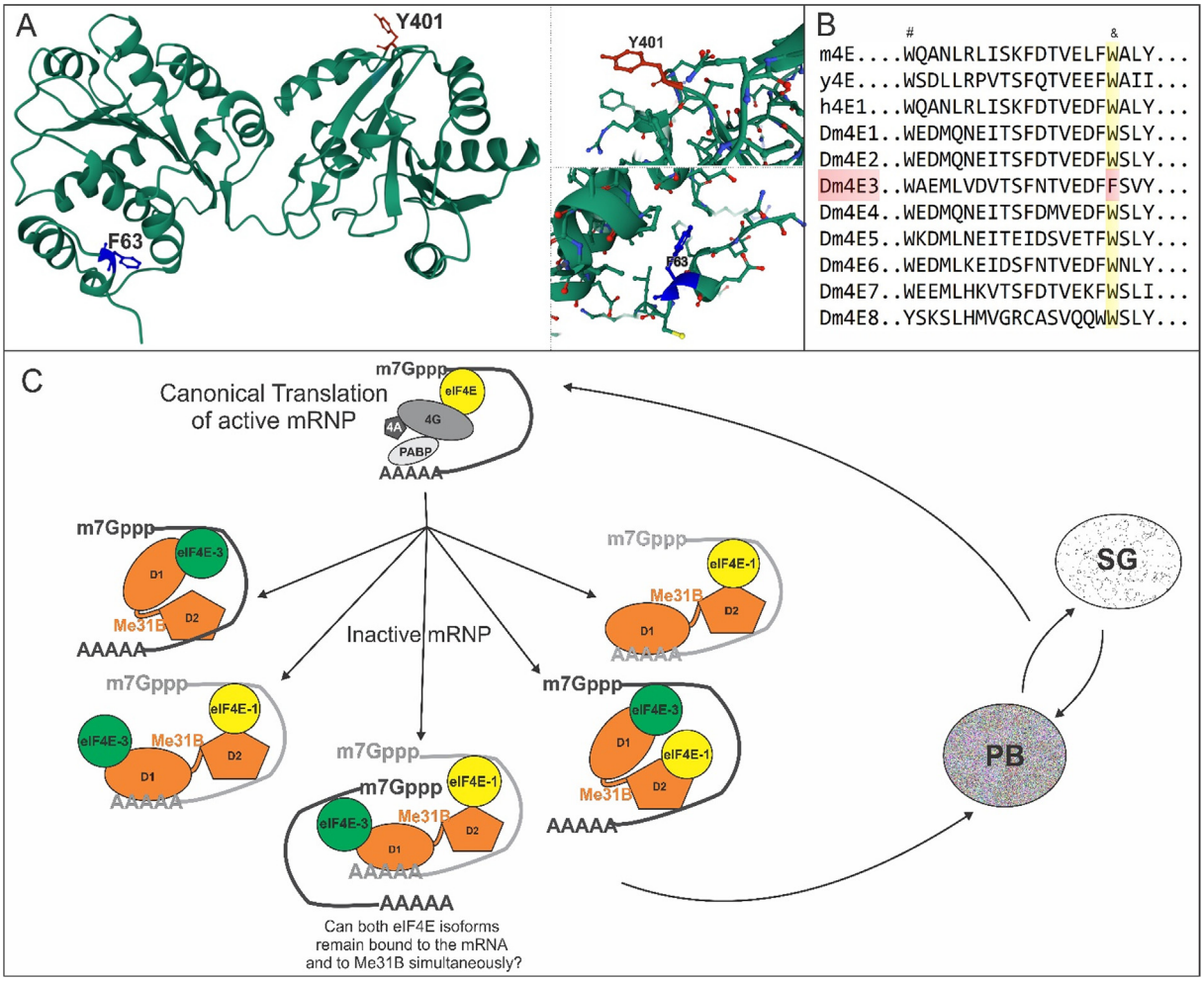

Figure 8. (A) Molecular modeling of Me31B. The residues required for the interaction with eIF4E. F63 (blue, lower right panel) is essential for eIF4E-3 interaction, and it is exposed in N-terminus at the D1 domain. Y401 (red, upper right panel) is required for eIF4E-1 interaction at the C-terminus at the D2 domain. Both residues are exposed to the surface and are able to interact with other proteins. They are far apart and would allow simultaneous interactions**. (B) Sequence comparison of eIF4E region required for Me31B interaction.** The alignment of amino acid sequences of *Drosophila* eIF4E isoforms, mouse (m4E), yeast (y4E) and human eIF4E-1 (h4E1) shows that the tryptophan residue required for the cap recognition (#) is conserved in all but eIF4HP. The tryptophan residue involved in interaction with 4G and other 4E-eIF4E-interacting proteins is conserved in all, but replaced by phenylalanine in eIF4E-3 (&, highlighted). **(C)** A model of the possible configurations of Me31B- eIF4Es complexes in mRNPs. The Me31B- eIF4E complex can be part of mRNPs repressing specific subsets of mRNA. This complex could occur in different combinations – Me31B could either bind only one eIF4E isoform or both simultaneously. See the discussion for hypotheses on the function.

its lateral surface.[58] eIF4E-interacting proteins, such as *D. melanogaster* Mextli, use a third interaction motif (auxiliary motif) to interact with eIF4E-1.[59] Our data add up to the complexity of the interacting mRNP landscape showing isoform-specific independent binding sites within the same eIF4E-interacting protein. This unique feature makes Me31B the first protein so-far reported with such dual capabilities. This opens the path for new studies to understand this remarkable feature. The dual interaction would allow several potential ways of regulation (Figure 8(C)). The Me31B- eIF4E complex can be part of mRNPs repressing specific subsets of mRNA. However, RNA might not be required for the interaction, as it has been shown for vertebrate ortholog ddx6/p54[14] and we have shown here.

eIF4E-Me31B complexes could occur in different combinations - Me31B might either bind only one eIF4E isoform or both simultaneously. In the latter, the two isoforms could remain bound to the mRNA to be silenced and should require the coexpression of the isoforms. We have shown that Me31B is expressed in testis, from the stem cells niche to spermatocytes. Jensen et al. showed that it does not colocalize with vasa in the nuage of stem cells, however, we observed colocalization in the cytoplasm. According to Jensen et al. Me31B controls male stem cell dedifferentiation and regulates *nanos* mRNA translation.[39] We did not detect expression of eIF4E-3 in stem cells, therefore, this interaction should be mediated by eIF4E-1. It is plausible to consider that in the stem cell niche, the interaction is binary and consistent with the lack of stem cell differentiation in me31B mutants[39] and with the fact that absence of eIF4E-1 is cellular lethal.[56] Later on in spermatogenesis, the spermatocytes express Me31B and both, eIF4E-1 and eIF4E-3, which implies that either binary or ternary complexes might form. If this is the case, it remains to be investigated. However, the facts that eIF4E-3 phenotype affects meiosis and that we observed accumulation of Me31B and eIF4E-3 in meiotic figures suggest that the interaction might reflect the function. A genetic dissection of me31B phenotypes and the effect of the interaction with any eIF4E isoform at this stage is not possible, because the lack of me31B blocks the progression of the germ line to spermatocytes. eIF4E-1 and eIF4E-3 simultaneous interaction with Me31B might occur leading to a different function than the binary complexes. These functions might imply still unknown mechanisms, not necessarily at the translational level. This is speculative, but constitutes our hypotheses based on the genetic, expression, and interaction data.

We support the idea that the regulatory capacity of Me31B depends on the various interactors and different biological contexts in which it happens. It represents another example of the diversity of the mRNA translation/silencing mechanism described up to now.[60] The results described here and the previous evidence from us and other laboratories further support the notion of the plasticity for the eIF4E interaction network, which confers unique properties to the different assembled mRNPs. The analysis of the function and structure of the Me31B/eIF4E interaction will shed light on this combinatorial regulation mechanism.

Experimental procedures

Cell culture and transfections

Drosophila S2 cells were grown on glass coverslips (Fisher Scientific) in Schneider's medium (Sigma, USA), supplemented with 10% fetal bovine serum (Natocor, Córdoba, Argentina) and 1% antibiotic–antimycotic mixture (Invitrogen, USA) at 28 °C. Plasmid transfections were performed after cells had reached ~90% confluency using Lipofectamine reagent (Roche), as recommended by the manufacturer. Sixteen hours after transfection, cells were washed with PBS (130 mM NaCl, 20 mM potassium phosphate, pH 7.4), fixed for 20 min with PBS pH 7.4/4% w/v paraformaldehyde, and mounted in antifade (Mowiol, Calbiochem).

Immunofluorescence

Cells were fixed as described above, washed with PBS pH 7.4, and permeabilized in PBS pH 7.4/0.2% Triton X-100 (Sigma) for 20 min. Cells were then rinsed with PBS, blocked in PBS pH 7.4 / 10% fetal calf serum (FCS) for 30 min, and incubated with the primary antibody diluted in PBS pH 7.4/10% FCS for 60 min. Subsequently, cells were washed with PBS pH 7.4 (4 × 15 min) and incubated with the secondary antibody in PBS pH 7.4 / 10%FCS for 45 min. Cells were again washed with PBS pH 7.4 (3 × 10 min) and mounted in antifade (Mowiol, Calbiochem).

Confocal laser scanning microscopy

Before imaging, cells were counterstained with DAPI and analyzed by epifluorescence to assess cell integrity. Images were acquired with a Carl Zeiss LSM 510-Meta confocal microscope using Argon (588/514 nm) and Helium/Neon (543/633 nm) lasers. The images were analyzed using the LSM software and Image J (https://rsbweb.nih.gov/ij/).

The following primary antibodies were used in this study: rabbit anti-rck/p54 (DDX6, Bethyl Laboratories; 1:500); rabbit anti-eIF4E-1 1:1000[61]; rabbit polyclonal affinity-purified anti-eIF4E-3 antibodies #967 and #968 1:300 (Biomatik, Ontario, Canada,[41] anti-GW182 and anti-TIA-1 (AbCam, Cambridge, UK; 1:500). The following secondary antibodies were used: anti-mouse, anti-goat, and anti-rabbit antibodies conjugated to Cyanine dyes (Jackson Inc.; 1:2000).

Colocalization analysis

Colocalization was analyzed using JACoP plugins (ImageJ software). New images were created by thresholding the background corrected images. The background corrected image from channel A (Me31B) was combined with the image for channel B (GW-182, TIA-1, 4E1, 4E3, 4E2 or 4EHP). The percent of colocalization was measured by taking the volume of Me31B signal that overlapped with the protein marker in the other channel and dividing it by the total volume of Me31B in the sample. Manders coefficient 1 (MA) represents the fraction of pixels that colocalize of the total pixels in channel A. In the same manner MB coefficient represent the fraction of pixels that colocalize of the total pixels in channel B.[62]

Acceptor photobleaching FRET

All data were obtained on an LSM 510 Meta (Zeiss). Samples were fixed with 4% PFA for 15 min and images acquired with a CAPOCHROMAT 63×/1.4 W Korr objective (Zeiss). Specific excitation and emission of the CFP-fusion proteins were effected by excitation at 458 nm with a 30 mW Argon/2 laser (AOTF transmission 15%) and collection of emitted light with a 475/525 nm bandpass filter. No emission from YFP fusion proteins was detected in this channel. CFP images were taken before and after photobleaching of the YFP signal using the same sensitivity settings. YFP signals were photobleached by full-power excitation at 514 nm with a 50-mW solid-state laser. Images of YFP-fusion proteins were obtained before and after photobleaching by excitation with a 30-mW Argon/2 laser (transmission 15%) at 514 nm excitation and emission collected from 530 nm bandpass filter (LSM 510 Meta Detector, Zeiss). No photobleaching of the CFP signal was observed under > 90% photodestruction of the YFP signal. The FRET efficiency[63] was determined for each PB separately by: Eap = (ID0- ID)/ ID0; with ID0 and ID denoting the sum of the respective pre- and post-bleach donor intensity in a PB.

Immunohistochemistry of Trap-line GFP-Me31B flies

y1 w1118; P(PTT-GB)hme31 BCB05282 fly stock was obtained from the Bloomington *Drosophila* Stock Center. Testes were dissected on ice in S2 Schneider's medium supplemented with 10% fetal bovine serum. The medium was removed, and testes were fixed in fixer solution [200 μl of 4% paraformaldehyde in PBST (PBS with 0.2%Tween 20), 600 μl heptane and 20 μl DMSO] for 20 minutes with slow rotation. The fixer was removed, and testes were washed three times for 15minutes each in 1.5 ml PBST followed by 1–2 hours blocking with 1 ml blocking solution (PBST, 0.1% Triton X-100, 1% BSA). Testes were incubated either with primary antibodies in blocking solution at 4 °C overnight, washed for 30 minutes in PBST, blocked for 30 minutes with 500 μl blocking solution containing 1% goat serum, and incubated with secondary antibodies in 500 μl blocking solution containing 8% goat serum overnight at 4 °C. At this step, testes were counterstained with DAPI (1 ng/ml) for 5 minutes, washed four times for 15 minutes each with 1.5 ml PBST, and mounted for imaging.

Plasmids construction

We generated plasmids encoding the YFP and CFP fusion proteins. *Drosophila* eIF4E-1 (FlyBase CG4035), eIF4E-2 (FlyBase CG4035), eIF4E-3 (FlyBase CG 8023), d4E-HP (FlyBase CG33100)[34,38] and Me31B (FlyBase CG4916).[28] cDNAs were PCR-amplified and cloned as EcoRI-EcoRI fragments onto the Topo Blunt vector (Invitrogen). cDNAs were PCR-re-amplified and finally subcloned into Hind III site of the pEYFP-C1 or pECFP-C1 vectors (Clontech).

Drosophila eIF4E-1 and eIF4E-3 cDNAs[34] were cloned into the pOBD2 vector[64] in-frame with the DNA-binding domain sequence of GAL4 to create the "bait" constructs. Me31B, 4E-BP (CG8846;[65] and PABP (CG5119;[66] were cloned into the activator domain sequence of GAL4 to generate the "prey" constructs. Me31B and 4E-BP were cloned into pGAD424 vector and PABP into pACT2 vector. See Table S3 for a complete list of the plasmids used in this work.

Site-directed mutagenesis of Me31B, eIF4E-1 and eIF4E-3 was carried out on the plasmids pOBD-eIF4E1 to change tryptophan 117 to alanine, and pOBD-eIF4E-3 was used to change Phenylalanine 103 to alanine. PCR amplification of each template was performed using 2X iProof master mix (Bio-Rad) with primers described in Ferrero et al. (2012).[8] The same protocol was used to mutate pGAD424-Me31B with the following primers (for more details, see Table S3):

Me31B^{F63A}r: CTTTTAAGGCAAGCCTCCTCGAA.
Me31B^{F63A}f: TTCGAGGAGGCTTGCCTTAAAAG.
Me31B^{L70R}r: GAATATACCCATACGCAGTTCTC.
Me31B^{L70R}f: GAGAACTGCGTATGGGTATATTC.
Me31B^{V366STOP}r: AATTGATTACTTAATTCACGGC.
Me31B^{V366STOP}f: GCCGTGAATTAAGTAATCAATT.
Me31B^{K251STOP}r: GCGTAAATGTTACTCCATGAA.
Me31B^{K251STOP}f: TTCATGGAGTAACATTTACGC.
Me31B^{Y401A}f: CTGATAACCGCCGAGGATCGGTT.
Me31B^{Y401A}r: AACCGATCCTCGGCGGTTATCA.
Me31B^{L407R}f: CGGTTTGATCGGCATCGGATTGA.
Me31B^{L407R}r: TCAATCCGATGCCGATCAAACCG.

Drosophila Me31B, eIF4E-1 and eIF4E-3 full open reading frames were cloned into the bacterial expression vector pKNE001 (a modified version of pET-SUMO, gift from Kolja

Eckermann,[67] in-frame with His-tag and a SUMO domain. Both vector and ORFs were PCR amplified using Q5 polymerase (New England Biolabs). Amplimers of the ORF were phosphorylated using polynucleotide kinase and blunt-end ligated to the non-phosphorylated vector. All expression fusions were fully sequenced.

pETSUMOr: GCCGCTGCCGTGATGATGATG.
pETSUMOf: TGAGATCCGGCTAACAAAG.
me31B-ATGf: ATGATGACTGAAAAGTTAAATTC.
me31B-STOPr: TTATTTGCTAACGTTGCCCTC.
eIF4E1-ATGf:
ATGCAGAGCGACTTTCACAGAATG.
eIF4E1-STOPr:
CTACAAAGTGTAGATCGATTTCACTT.
eIF4E3-ATGf: ATGGTGTACACCGGTTACGTAAG.
eIF4E3-STOPr:
CTACAATGTGTAGATGGCATTGAC.

Yeast two hybrid assay

Interactions between "bait" and "prey" proteins were detected following a yeast interaction-mating method using the strains PJ69-4a and PJ69-4alpha (Table S2).[64] Diploid cells containing both bait and prey plasmids were grown in selective media (–Trp, –Leu) and shown as growth control. Protein interactions were detected by replica-plating diploid cells onto selective media (–Trp, Leu, His) containing 3-amino-1,2,4-triazole (3AT). Growth was scored after four days of growth at 30 °C.

The 3AT amount was titrated within a range of 0, 10, 12, 15, 20, and 30 mM of 3AT, resulting in 12 mM the minimum concentration needed to inhibit background growth and still enable the positive growth controls.

Co-immunoprecipitation assay

100–150 testis were dissected in ice cold PBS and after brief centrifugation resuspended in 300 μl lysis buffer (25 mM HEPES pH 7.4, 100 mM NaCl, 0.5% Triton X-100, 0,3% NP-40, 0.5 mM EDTA, 10% glycerol and protease inhibitors Complete-Roche). The tissue was homogenized in a 1 ml glass-glass Dounce homogenizer. The homogenate was centrifuged for 10 minutes at 15,000 g and 4 °C. The supernatant was incubated with 20 μl of GFP-Trap magnetic beads (chromotek) for 8 hours at 4 °C. The beads were separated and washed three times with ice cold 100 mM NaCl buffer (25 mM HEPES pH 7.4, 100 mM NaCl, 0,1% Triton X-100, 0.5 mM EDTA, 10% glycerol) and twice with 150 mM NaCl buffer (25 mM HEPES pH 7.4, 150 mM NaCl, 0,1% Triton X-100, 0.5 mM EDTA, 10% glycerol). The washed beads were resuspended in 1X SDS-PAGE sample buffer, boiled for 5 minutes and the proteins separated in a 4–25% gradient gel (BioRad) and transferred to a nitrocellulose membrane. eIF4E-3 was revealed using rat anti-eIF4E-3 antibody.[42]

2×10^7 *D. melanogaster* S2 cells were collected of a 25 cm^2 flask and after brief centrifugation resuspended in ice cold 400 μl lysis buffer (150 mM NaCl, 50 mM Tris-HCl pH 8.0, 1% NP40 and protease inhibitors Complete, Roche). The cell lysate was centrifuged for 10 minutes at 17,000 g at 4 °C. The supernatant was incubated with 25 μl of Dynabeads Protein G (Life Technology) pre-incubated with anti-eIF4E-1[61] with rotation for 10 min at room temperature for 2 hours at 4 °C. The beads were separated and washed three times with ice cold Wash Buffer (150 mM NaCl, 10 mM Tris-HCl pH 7,5, 0,5mM EDTA). The bound proteins were eluted with glycine 0,2M, separated in a 4–25% gradient gel and transferred to nitrocellulose membrane (Schleicher & Schuell). eIF4E-3 was revealed using rabbit anti-eIF4E-3 antibody[42] and Me31B using rabbit anti-DDX6 (Abcam).

Recombinant protein expression, purification and interaction assay

The plasmids pHis-SUMO-me31B, pHis-SUMO-4E1 and pHis-SUMO-4E3 were transformed into BL21-CodonPlus-RIL (Agilent Technologies) for recombinant protein expression. The bacteria grew at 37 °C until A_{600} = 0.7, transferred to 16 °C and induced with 1 mM IPTG for 24 hours. The bacteria were isolated by centrifugation at 5,000*g* 10 minutes and the pellet resuspended in lysis buffer (50 mM phosphate pH 8.0; 400 mM NaCl, 1 μg/ml Lysozyme, 10μg/ml RNAse, 10 μg/ml benzonase and 1% Triton X-100), sonicated and the lysate clarified at 25.000xg 30 min. eIF4E-1 and eIF4E-3 were purified in Nickel-agarose (Quiagen) in a gradient of 25–300 mM imidazole in native conditions. Me31B was present in inclusion bodies and purified in denaturing conditions (50 mM phosphate pH 8.0; 400 mM NaCl; 8 M urea) in Nickel-agarose and eluted in a gradient of 25–300 mM imidazole. The recombinant proteins were dialyzed against 25 mM phosphate pH 8.0; 200 mM NaCl; 1 mM DTT; 10% glycerol and stored frozen in aliquots. The His-SUMO tag was removed by digesting 20 μg of recombinant protein with SUMO protease (Sigma-Aldrich, Germany) as recommended by the manufacturers. The purity of the proteins was assessed by SDS-PAGE and Coomassie staining as >90%.

50 μg of recombinant, purified His-tagged eIF4E-1 was bound to 100 μl of Ni-TA-Agarose (Quiagen, Germany) and washed twice in Binding Buffer (25 mM Phosphate pH8; 200 mM NaCl; 1 mM DTT; 10% glycerol; 25 mM imidazol). 10 μl of settled eIF4E-1-beads were incubated for 60 minutes at 4 °C with 2–5 μg of recombinant, untagged, Me31B and eIF4E-3 in buffer 25 mM HEPES pH 7.4, 100 mM NaCl, 0,1% Triton X-100,

1 mM DTT, 10% glycerol. The beads were washed twice with the same buffer containing 150 mM NaCl and the pelleted beads were resuspended in 1X SDS-PAGE sample buffer, boiled for 5 minutes and the proteins separated in a 4–12% gradient gel (NuPAGE Invitrogen). The copurified proteins were revealed by silver staining.

Me31B molecular modelling

Starting structures were generated first by constructing homology models of Me31B based on the DDX6 structure (PDB: 4CT5) using SWISS-MODEL.[68] Simulation analysis was performed using RCSB Protein Data Bank (https://www.rcsb.org/). For more information see supplemental material.

Acknowledgements

We thank Paul Lasko (McGill University, Canada) for the generous gift of *Drosophila* anti-eIF4E-3 antibodies. R.R.P thanks Herbert Jäckle and Gerd Vorbruggen (Max Planck Institute for Multidisciplinary Sciences, Germany) for discussions and suggestions.

Author contributions

Conceived and designed the experiments: C.L. and R.R.P. Performed the experiments: R.R.P., G.C., E.V. and C.L. Analyzed the data: C.L., R.R. P and G.H. Contributed reagents/materials/analysis tools: C.L., G.H and R.R.P. Wrote the paper: G.H., R.R.P. and C.L.

Funding and additional information

C.L. and R.R.P. are investigators and E.S.V. is a doctoral fellow of CONICET, Argentina. This work was supported by grants of ANPCyT (PICT-2016-2045 to C.L. and PICT-2015-2128 to R.R.P.) and the Alexander von Humboldt Research Award and Gauss Professorship Award (R.R.P.) G.H. was supported by the intramural funding program of the National Institute of Cancer (Instituto Nacional de Cancerología, INCan), Mexico.

Conflict of Interest

The authors declare that they have no conflicts of interest with the contents of this article.

Appendix A. Supplementary material

Supplementary material to this article can be found online at https://doi.org/10.1016/j.jmb.2023.167949.

Received 12 November 2021;
Accepted 3 January 2023;
Available online 10 January 2023

Keywords:
translation control;
mRNP;
translation initiation;
P-bodies;
male germ line

† Present address: Michroma, Montevideo 3371, S2002 Rosario, Argentina.
‡Present address: Administración Nacional de Medicamentos, Alimentos y Tecnología Médica (ANMAT), Av. de Mayo 869, C1084AAD-Buenos Aires, Argentina.

References

1. Hershey, J.W.B., Sonenberg, N., Mathews, M.B., (2018). Principles of translational control. *Cold Spring Harb. Perspect. Biol.*, a032607.
2. Maier, T., Guell, M., Serrano, L., (2009). Correlation of mRNA and protein in complex biological samples. *FEBS Lett.* **583**, 3966–3973.
3. Tauber, D., Tauber, G., Parker, R., (2020). Mechanisms and Regulation of RNA Condensation in RNP Granule Formation. *Trends Biochem. Sci.* **45**, 764–778.
4. Decker, C.J., Parker, R., (2012). P-bodies and stress granules: possible roles in the control of translation and mRNA degradation. *Cold Spring Harb. Perspect. Biol.* **4**, a012286
5. Layana, C., Corujo, G.H., Rivera-Pomar, R.V., (2016). Ribonucleoprotein foci in eukaryotes: How to translate the silence. In: Hernández, G., Jagus, R. (Eds.), *Evolution of the protein synthesis machinery and its regulation*. Springer, Switzerland, pp. 491–511.
6. Buchan, J.R., (2014). mRNP granules. Assembly, function, and connections with disease. *RNA Biol.* **11**, 1019–1030.
7. Brengues, M., Teixeira, D., Parker, R., (2005). Movement of eukaryotic mRNAs between polysomes and cytoplasmic processing bodies. *Science* **310**, 486–489.
8. Ferrero, P.V., Layana, C., Paulucci, E., Gutiérrez, P., Hernández, G., Rivera-Pomar, R.V., (2012). Cap binding-independent recruitment of eIF4E to cytoplasmic foci. *BBA* **1823**, 1217–1224.
9. Kedersha, N., Stoecklin, G., Ayodele, M., Yacono, P., Lykke-Andersen, J., Fritzler, M.J., Scheuner, D., Kaufman, R.J., et al., (2005). Stress granules and processing bodies are dynamically linked sites of mRNP remodeling. *J. Cell Biol.* **169**, 871–884.
10. Ferraiuolo, M.A., Basak, S., Dostie, J., Murray, E.L., Schoenberg, D.R., Sonenberg, N., (2005). A role for the eIF4E-binding protein 4E-T in P-body formation and mRNA decay. *J. Cell Biol.* **170**, 913–924.
11. Andrei, M.A., Ingelfinger, D., Heintzmann, R., Achsel, T., Rivera-Pomar, R., Lührmann, R., (2005). A role for eIF4E and eIF4E-transporter in targeting mRNPs to mammalian processing bodies. *RNA (New York, N.Y.)* **11**, 717–727.
12. Frydryskova, K., Masek, T., Borcin, K., Mrvova, S., Venturi, V., Pospisek, M., (2016). Distinct recruitment of human

eIF4E isoforms to processing bodies and stress granules. *BMC Mol. Biol.* **17**, 21.
13. Akao, Y., Matsumoto, K., Ohguchi, K., Nakagawa, Y., Yoshida, H., (2006). Human DEAD-box/RNA unwindase rck/p54 contributes to maintenance of cell growth by affecting cell cycle in cultured cells. *Int. J. Oncol.* **29**, 41–48.
14. Minshall, N., Standart, N., (2004). The active form of Xp54 RNA helicase in translational repression is an RNA-mediated oligomer. *Nucleic Acids Res.* **32**, 1325–1334.
15. Kramer, S., Bannerman-Chukualim, B., Ellis, L., Boulden, E.A., Kelly, S., Field, M.C., Carrington, M., (2013). Differential localization of the two T. brucei poly(A) binding proteins to the nucleus and RNP granules suggests binding to distinct mRNA pools. *PLoS One* **8**, e54004.
16. Rouhana, L., Shibata, N., Nishimura, O., Agata, K., (2010). Different requirements for conserved post-transcriptional regulators in planarian regeneration and stem cell maintenance. *Dev. Biol.* **341**, 429–443.
17. Berengues, M., Parker, R., (2007). Accumulation of polyadenylated mRNA, Pab1p, eIF4E, and eIF4G with P-bodies in Saccharomyces cerevisiae. *Mol. Biol. Cell* **18**, 2592–2602.
18. Hoyle, N.P., Castelli, L.M., Campbell, S.G., Holmes, L.E., Ashe, M.P., (2007). Stress-dependent relocalization of translationally primed mRNPs to cytoplasmic granules that are kinetically and spatially distinct from P-bodies. *J. Cell Biol.* **179**, 65–74.
19. McCambridge, A., Solanki, D., Olchawa, N., Govani, N., Trinidad, J.C., Gao, M., (2020). Comparative proteomics reveal Me31B's interactome dynamics, expression regulation, and assembly mechanism into germ granules during *Drosophila* germline development. *Sci. Rep.* **10**, 564.
20. Rieckher, M., Markaki, M., Princz, A., Schumacher, B., Tavernarakis, N., (2018). Maintenance of proteostasis by P body-mediated regulation of eIF4E availability during aging in *Caenorhabditis elegans*. *Cell Rep.* **25**, 199–211.e196.
21. Merrick, W.C., (2015). eIF4F: a retrospective. *J. Biol. Chem.* **XX**, XXX.
22. Pelletier, J., Sonenberg, N., (2019). The organizing principles of eukaryotic ribosome recruitment. *Annu. Rev. Biochem.* **88**, 307–335.
23. Borden, K.L., (2016). The eukaryotic translation initiation factor eIF4E wears a "cap" for many occasions. *Translation (Austin)* **4**, e1220899.
24. Christie, M., Igreja, C., (2021). eIF4E-homologous protein (4EHP): a multifarious cap-binding protein. *FEBS J.*.
25. Lasko, P., (2000). The *Drosophila melanogaster* genome: translational factors and RNA binding proteins. *J. Cell Biol.* **150**, F51–F56.
26. Weston, A., Sommerville, J., (2006). Xp54 and related (DDX6-like) RNA helicases: roles in messenger RNP assembly, translation regulation and RNA degradation. *Nucleic Acids Res.* **34**, 3082–3094.
27. Thomson, T., Liu, N., Arkov, A., Lehmann, R., Lasko, P., (2008). Isolation of new polar granule components in *Drosophila* reveals P body and ER associated proteins. *Mech. Dev.* **125**, 865–873.
28. Wetson, A., Sommerville, J., (2006). Xp54 and related (DDX6-like) RNA helicases: roles in messenger RNP assembly, translation regulation and RNA degradation. *Nucleic Acid Res.* **34**, 3082–3094.
29. DeHaan, H., McCambridge, A., Armstrong, B., Cruse, C., Solanki, D., Trinidad, J.C., Arkov, A., Gao, M., (2017). An *in vivo* proteomic analysis of the Me31B interactome in *Drosophila* germ granules. *FEBS Lett.* **591**, 3536–3547.
30. Nakamura, A., Amikura, R., Hanyu, K., Kobayashi, S., (2001). Me31B silences translation of oocyte-localizing RNAs through the formation of cytoplasmic RNP complex during Drosophila oogenesis. *Development (Cambridge, England)* **128**, 3233–3242.
31. Wang, M., Ly, M., Lugowski, A., Laver, J.D., Lipshitz, H.D., Smibert, C.A., Rissland, O.S., (2017). ME31B globally represses maternal mRNAs by two distinct mechanisms during the *Drosophila* maternal-to-zygotic transition. *eLife* **6**, e27891.
32. Liu, L., Qi, H., Wang, J., Lin, H., (2011). PAPI, a novel TUDOR-domain protein, complexes with AGO3, ME31B and TRAL in the nuage to silence transposition. *Development (Cambridge, England)* **138**, 1863–1872.
33. Layana, C., Ferrero, P., Rivera-Pomar, R., (2012). Cytoplasmic ribonucleoprotein foci in eukaryotes: hotspots of bio(chemical) diversity. *Comp. Funct. Genom.* **2012**, 504292
34. Schneider, I., (1972). Cell lines derived from late embryonic stages of Drosophila melanogaster. *J. Embryol. Exp. Morphol.* **27**, 353–365.
35. Buchan, J.R., Muhlrad, D., Parker, R., (2008). P bodies promote stress granule assembly in Saccharomyces cerevisiae. *J. Cell Biol.* **183**, 441–455.
36. Buchan, J.R., Parker, R., (2009). Eukaryotic stress granules: the ins and outs of translation. *Mol. Cell* **36**, 932–941.
37. Hernández, G., Altmann, M., Sierra, J.M., Urlaub, H., Corral, R.D., Schwartz, P., Rivera-Pomar, R., (2005). Functional analysis of seven genes encoding eight translation initiation factor 4E (eIF4E) isoforms in *Drosophila*. *Mech. Dev.* **122**, 529–543.
38. Zabolotskaya, M.V., Grima, D.P., Lin, M.D., Chou, T.B., Newbury, S.F., (2008). The 5'-3' exoribonuclease Pacman is required for normal male fertility and is dynamically localized in cytoplasmic particles in Drosophila testis cells. *Biochem. J* **416**, 327–335.
39. Jensen, L., Venkei, Z.G., Watase, G.J., Bisai, B., Pletcher, S., Lee, C.Y., Yamashita, Y.M., (2021). me31B regulates stem cell homeostasis by preventing excess dedifferentiation in the Drosophila male germline. *J. Cell Sci.* **134**
40. Nakamura, A., Sato, K., Hanyu-Nakamura, K., (2004). *Drosophila* Cup is an eIF4E binding protein that associates with Bruno and regulates *oskar* mRNA translation in oogenesis. *Dev. Cell* **6**, 69–78.
41. Hernández, G., Gandin, V., Han, H., Ferreira, T., Sonenberg, N., Lasko, P., (2012). Translational control by *Drosophila* eIF4E-3 is essential for cell differentiation during spermiogenesis. *Development (Cambridge, England)* **139**, 3211–3220.

42. Patterson, G.H., Piston, D.W., Barisas, B.G., (2000). Forster distances between green fluorescent protein pairs. *Anal. Biochem.* **284**, 438–440.
43. Miyawaki, A., Tsien, R.Y., (2000). Monitoring protein conformations and interactions by fluorescence resonance energy transfer between mutants of green fluorescent protein. *Methods Enzymol.* **327**, 472–500.
44. Wouters, F.S., Bastiaens, P.I., Wirtz, K.W., Jovin, T.M., (1998). FRET microscopy demonstrates molecular association of non-specific lipid transfer protein (nsL-TP) with fatty acid oxidation enzymes in peroxisomes. *EMBO J.* **17**, 7179–7189.
45. Mader, S., Lee, H., Pause, A., Sonenberg, N., (1995). The translation initiation factor eIF-4E binds to a common motif shared by the translation factor eIF-4 gamma and the translational repressors 4E-binding proteins. *Mol. Cell Biol.* **15**, 4990–4997.
46. Cho, P.F., Poulin, F., Cho-Park, Y.A., Cho-Park, I.B., Chicoine, J.D., Lasko, P., Sonenberg, N., (2005). A new paradigm for translational control: inhibition via 5'-3' mRNA tethering by Bicoid and the eIF4E cognate 4E-HP. *Cell* **121**, 411–423.
47. Volpon, L., Culjkovic-Kraljacic, B., Osborne, M.J., Ramteke, A., Sun, Q., Niesman, A., Chook, Y.M., Borden, K.L., (2016). Importin 8 mediates m7G cap-sensitive nuclear import of the eukaryotic translation initiation factor eIF4E. *PNAS* **113**, 5263–5268.
48. White-Cooper, H., Schäfer, M.A., Alphey, L.S., Fuller, M.T., (1998). Transcriptional and post-transcriptional control mechanisms coordinate the onset of spermatid differentiation with meiosis I in Drosophila. *Development (Cambridge, England)* **125**, 125–134.
49. Ghosh, S., Lasko, P., (2015). Loss-of-function analysis reveals distinct requirements of the translation initiation factors eIF4E, eIF4E-3, eIF4G and eIF4G2 in *Drosophila* spermatogenesis. *PLoS One* **10**, e0122519.
50. Anderson, P., Kedersha, N., (2006). RNA granules. *J. Cell Biol.* **172**, 803–808.
51. Eulalio, A., Behm-Ansmant, I., Schweizer, D., Izaurralde, E., (2007). P-body formation is a consequence, not the cause, of RNA-mediated gene silencing. *Mol. Cell Biol.* **27**, 3970–3981.
52. Kugler, J.M., Lasko, P., (2009). Localization, anchoring and translational control of oskar, gurken, bicoid and nanos mRNA during Drosophila oogenesis. *Fly* **3**, 15–28.
53. Kugler, J.M., Chicoine, J., Lasko, P., (2009). Bicaudal-C associates with a Trailer Hitch/Me31B complex and is required for efficient Gurken secretion. *Dev. Biol.* **328**, 160–172.
54. Schäfer, M., Nayernia, K., Engel, W., Schäfer, U., (1995). Translational control in spermatogenesis. *Dev. Biol.* **172**, 344–352.
55. Coller, J., Parker, R., (2005). General translational repression by activators of mRNA decapping. *Cell* **122**, 875–886.
56. Hernández, G., Vazquez-Pianzola, P., (2005). Functional diversity of the eukaryotic translation initiation factors belonging to eIF4 families. *Mech. Dev.* **122**, 865–876.
57. Santalla, M., García, A., Mattiazzi, A., Valverde, C.A., Schiemann, R., Paululat, A., Hernández, G., Meyer, H., et al., (2022). Interplay between SERCA, 4E-BP, and eIF4E in the Drosophila heart. *PLoS One* **17**, e0267156.
58. Igreja, C., Peter, D., Weiler, C., Izaurralde, E., (2014). 4E-BPs require non-canonical 4E-binding motifs and a lateral surface of eIF4E to repress translation. *Nature Commun.* **5**, 4790.
59. Peter, D., Igreja, C., Weber, R., Wohlbold, L., Weiler, C., Ebertsch, L., Weichenrieder, O., Izaurralde, E., (2015). Molecular architecture of 4E-BP translational inhibitors bound to eIF4E. *Mol. Cell* **57**, 1074–1087.
60. Hernández, G., García, A., Sonenberg, N., Lasko, P., (2020). Unorthodox Mechanisms to Initiate Translation Open Novel Paths for Gene Expression. *J. Mol. Biol.* **432**, 166702
61. Maroto, F.G., Sierra, J.M., (1989). Purification and characterization of mRNA cap-binding protein from *Drosophila melanogaster* embryos. *Mol. Cell Biol.* **9**, 2181–2190.
62. Manders, E.M.M., Verbeek, F.J., Aten, J.A., (1993). Measurement of co-localization of objects in dual-colour confocal images. *J. Microsc.* **169**, 375–382.
63. Bastiaens, P., Majoul, I., Verveer, P., Soling, H., Jovin, T., (1996). Imaging the intracellular trafficking and state of the AB5 quaternary structure of cholera toxin. *EMBO J.* **15**, 4246–4253.
64. Cagney, G., Uetz, P., Fields, S., (2000). High-throughput screening for protein-protein interactions using two-hybrid assay. *Meth. Enzymol.* **328**, 3–17.
65. Miron, M., Verdú, J., Lachance, P.E., Birnbaum, M.J., Lasko, P.F., Sonenberg, N., (2001). The translational inhibitor 4E-BP is an effector of PI(3)K/Akt signalling and cell growth in *Drosophila*. *Nat. Cell Biol.* **3**, 596–601.
66. Vazquez-Pianzola, P., Urlaub, H., Suter, B., (2011). Pabp binds to the osk 3'UTR and specifically contributes to osk mRNA stability and oocyte accumulation. *Dev. Biol.* **357**, 404–418.
67. Farnworth, M.S., Eckermann, K.N., Bucher, G., (2020). Sequence heterochrony led to a gain of functionality in an immature stage of the central complex: A fly-beetle insight. *PLoS Biol.* **18**, e3000881.
68. Waterhouse, A., Bertoni, M., Bienert, S., Studer, G., Tauriello, G., Gumienny, R., Heer, F.T., de Beer, T.A.P., et al., (2018). SWISS-MODEL: homology modelling of protein structures and complexes. *Nucleic Acids Res.* **46**, W296–W303.